Hindawi Publishing Corporation
Advances in Materials Science and Engineering
Volume 2016, Article ID 9435431, 17 pages
http://dx.doi.org/10.1155/2016/9435431

Research Article

Modeling of Point Defects Annihilation in Multilayered Cu/Nb Composites under Irradiation

Sarah Fadda,[1,2] Antonio Mario Locci,[1] and Francesco Delogu[1]

[1]*Dipartimento di Ingegneria Meccanica, Chimica e dei Materiali, Università degli Studi di Cagliari, Via Marengo 2, 09123 Cagliari, Italy*
[2]*Centre for Process Systems Engineering, Department of Chemical Engineering, Imperial College London, London SW7 2AZ, UK*

Correspondence should be addressed to Antonio Mario Locci; antonio.locci@dimcm.unica.it

Received 15 July 2015; Accepted 16 December 2015

Academic Editor: Markku Leskela

This work focuses on a mathematical modeling of the response to irradiation of a multilayer composite material. Nonstationary balance equations are utilized to account for production, recombination, transport, and annihilation, or removal, of vacancies and interstitials at interfaces. Although the model developed has general validity, Cu/Nb multilayers are used as case study. Layer thickness, temperature, radiation intensity, and surface recombination coefficients were varied systematically to investigate their effect on point defect annihilation processes at interfaces. It is shown that point defect annihilation at interfaces mostly depends on point defect diffusion. The ability of interfaces to remove point defects can be described by a simple map constructed using only two dimensionless parameters, which provides a general tool to estimate the efficiency of vacancy and interstitial removal in multilayer composite materials.

1. Introduction

Intense irradiation, high temperature, high mechanical stresses, and the presence of chemically aggressive fluids make nuclear environment extreme [1, 2]. Under these conditions, materials undergo significant degradation processes that definitely limit their reliability, lifetime, and efficiency [2–10].

Point defect supersaturation due to ballistic atomic displacements induced by irradiation and the consequent generation of sustained net fluxes of vacancies and interstitials play a major role in the progressive damaging of the material [11, 12]. Biased production and annihilation of point defects depress recombination processes, allowing them time for clustering and nucleating voids [12]. Furthermore, interaction of vacancies with He atoms generated by neutron-activated transmutation reactions finally results in the precipitation of He bubbles [4, 9, 13]. These contribute to material embrittlement and hardening, typically accompanied by dimensional and chemical instabilities as well as by swelling, solute redistribution, creep, and associated processes [2, 4–7, 11–23].

Contrasting degradation processes and eventually enhancing the radiation tolerance of materials represent a stringent need in view of the increasing energy demand worldwide and the unsatisfactory development degree attained by massive energy production related to renewable sources. At the same time, improving radiation resistance poses a tremendous challenge to materials scientists and technologists addressing future fission and fusion reactors [11, 24–29].

In principle, a high density of unbiased radiation-induced point defect sinks could absorb, and annihilate, vacancy and interstitials by facilitating the recombination of Frenkel pairs [6, 10, 12, 13, 22, 30, 31]. In this respect, surfaces, grain boundaries, and interphase boundaries have attracted most interest [6, 21, 27, 32–37]. Due to the characteristic high densities of grain boundaries, nanostructured materials have recently gained much attention [10, 12, 20, 22, 23, 28, 38, 39]. Excess free volume and higher diffusivity of defects at grain boundaries, combined with shorter diffusion distances of point defects to interfaces, enhance, indeed, recombination probabilities [2, 4, 34, 37]. However, the use of nanostructured

materials requires maintaining a high density of interfaces and grain boundaries during prolonged irradiation [39], which is not an easy task due to the thermal instability of nanocrystalline grains and their tendency to coarsen rapidly even at modest temperatures [28, 40, 41].

In this regard, a possible engineering strategy involves using multiphase nanostructured materials [6, 22, 42]. In particular, multilayer composites can be designed to exhibit enhanced radiation tolerance [6, 11, 20, 42–45]. For example, Cu/Nb nanolayered composites have been shown to possess satisfactory dimensional, chemical, and microstructural stability over a wide range of irradiation conditions [6, 7, 11, 37, 42, 46]. This is mostly due to the positive heat of mixing of Cu and Nb, which exhibit only terminal solid solubility and no tendency to form intermetallic compounds [11, 28].

The mechanisms underlying point defect annihilation at Cu/Nb interfaces have been studied recently by density functional theory (DFT) [47], molecular dynamics [1, 11, 21, 27, 34, 35, 48], and phase field calculations [37]. This provided considerable detail on the atomistic processes taking place on relatively short time scales. Nevertheless, the overall mechanistic scenario remains largely unknown [23]. Within this context, developing a continuum approach to describe long-term evolution of point defects under irradiation conditions is highly desirable.

Aimed at providing a contribution along this line, the present work concerns the development and validation of a mathematical model in space and time *continuum* addressing the dynamic behavior of vacancies and interstitials during irradiation. Nanometer-sized Cu/Nb multilayer composites are used as case study. Interfaces are described as a continuum spatial distribution of either neutral or variable-biased sinks [49]. This allows modeling both noncoherent interfaces such as grain boundaries and incoherent precipitates, which typically behave like neutral sinks, and coherent and semicoherent interfaces, which behave like variable-biased sinks [49]. Nonstationary balance equations for vacancy and interstitials are used to describe production, recombination, transport, and annihilation, or removal, of point defects at interfaces. Layer thickness, temperature, radiation conditions, and surface recombination coefficients were varied systematically to investigate their effect on annihilation processes at interfaces.

The numerical findings show that the kinetics of point defect annihilation at interfaces mostly depend on their diffusion into the material volume, whereas boundary structure plays a minor role. Furthermore, interfaces exhibit a capability of point defect removal amenable to simple description based on a map constructed using two parameters, namely, dimensionless vacancy diffusivity and the ratio between the characteristic times of point defect recombination and production. Such maps provide a general tool to estimate the efficiency of vacancy and interstitial removal and can be utilized for investigating the behavior of any given multilayer composite material.

2. Mathematical Model

In this work, it is assumed that interfaces between materials are capable of adsorbing point defects. It is also assumed that there are no crossings of defects between interfaces and that distribution of defects on the interfaces is not spatially dependent. On the other hand, defect concentrations inside the layers are assumed to be dependent only upon the distance from the interfaces. Under these hypotheses, multilayer composite systems may be analyzed in one spatial coordinate adopting a simple reaction-diffusion model of a single layer bounded by two interfaces. The latter ones are assumed in this work to be perfectly stable under irradiation. This assumption means that intermixing is negligible and thus that the proposed model applies to those systems whose alternate layers are constituted by mutually immiscible elements.

The model takes into account the formation of Frenkel pairs at a constant and spatially uniform rate, as well as their diffusion and mutual annihilation. Radiation-induced vacancies and self-interstitial atoms are considered isolated; thus the formation of defect clusters like voids and dislocation loops is not taken into account. This simplifying assumption typically holds at low point defect concentrations because of the negligible cluster nucleation rate in these conditions. In addition, point defects annihilation at grain boundaries is also neglected. Interfaces are then the only sink for point defects taken into account in this model. This hypothesis is justified by experimental evidences in several multilayer composites [36]. In this regard, it should be pointed out that since clusters and grain boundaries act as sinks for point defects, the results of this model may be considered conservative in terms of point defect concentrations. In other words, the model outputs represent the maximum achievable point defect concentrations under the specified operating conditions.

The evolution of point defects concentration, that is, vacancies (v) and self-interstitial atoms (SIA) (i), is described by the following one-dimensional spatial reaction-diffusion equation,

$$\frac{\partial C_j}{\partial t} - D_j \frac{\partial^2 C_j}{\partial x^2} = K^0 - R^C \quad j = i, v, \tag{1}$$

along with its initial condition

$$\begin{aligned} t &= 0, \quad \forall x \\ C_j &= C_j^{\text{eq}} \quad j = i, v, \end{aligned} \tag{2}$$

where C_j is the concentration of the point defect of type j and D_j is the diffusion coefficient of the point defect of type j, while K^0 and R^C are the production and the recombination rates of Frenkel pairs per unit volume, respectively. The reader should refer to Nomenclature for the significance of the other symbols.

Diffusion coefficients are expressed in terms of Arrhenius form for thermally activated events as follows:

$$D_j = a^2 \alpha_j \nu_D \exp\left(\frac{S_j^M}{k_B}\right) \exp\left(-\frac{E_j^M}{k_B T}\right) \quad j = i, v. \tag{3}$$

The production rate of Frenkel pairs K^0 has been calculated using the Stopping and Range of Ions in Matter (SRIM)

technique and depends on radiation conditions and layer material lattice. The recombination rate of point defects is expressed as a second-order reaction:

$$R_j^C(x,t) = K_{iv}\left(C_i - C_i^{\mathrm{eq}}\right)\left(C_v - C_v^{\mathrm{eq}}\right) \quad j = i, v, \tag{4}$$

where the kinetic constant is given by

$$K_{iv} = \frac{\alpha_{iv}\Omega}{a^2}\left(D_v + D_i\right) \quad j = i, v. \tag{5}$$

C_j^{eq} is the concentration of the point defect of type j at thermodynamic equilibrium, that is, the concentration value at a given temperature in absence of radiation. It depends on temperature according to the following equation:

$$C_j^{\mathrm{eq}} = \frac{1}{\Omega}\exp\left(\frac{S_j^F}{k_B}\right)\exp\left(-\frac{E_j^F}{k_B T}\right) \quad j = i, v. \tag{6}$$

Boundary conditions for (1) should take into account the characteristics of interfaces. In particular, if we assumed a planar surface, in the case of neutral sinks, the boundary conditions may be expressed as [50]

$$\begin{gathered} x = 0, \quad x = L \quad \forall t \\ D_j\frac{\partial C_j}{\partial x} = K_j\left(C_j - C_j^{\mathrm{eq}}\right) \quad j = i, v, \end{gathered} \tag{7}$$

where L is the thickness of the layer. Under the assumption that the lattice is not severely distorted over the final jump region, the transfer velocity is equal to

$$K_j = \frac{D_j}{b} \quad j = i, v, \tag{8}$$

where b is the metal lattice spacing. It is worth pointing out that the boundary condition of a neutral sink can be alternately expressed as

$$\begin{gathered} x = 0, \quad x = L \quad \forall t \\ C_j = C_j^{\mathrm{eq}} \quad j = i, v, \end{gathered} \tag{9}$$

which coincides with the boundary condition of the so-called perfect sink.

In the case of interfaces acting as variable-biased sinks, boundaries are modeled considering a surface (interface) concentration of traps for vacancies, S_v^{tot}, and a surface (interface) concentration of traps for interstitials, S_i^{tot}. The occupation probability of traps of each type is taken to be f_v and f_i, respectively. An interstitial atom adjacent to the interface is assumed to be able to enter an unoccupied interstitial trap site or to recombine with the nearest neighbor trapped vacancy, jumping there from z possible adjacent sites in the matrix. Similar processes are possible for vacancies. Moreover, trapped interstitials and vacancies may recombine on interfaces. According to this picture, boundary conditions at interfaces acting as a variable-biased sink may be expressed as [50]

$$\begin{gathered} x = 0, \quad x = L \quad \forall t \\ D_j\frac{\partial C_j}{\partial x} = \left(1 - f_j + zf_k\right)K_j\left(C_j - C_j^{\mathrm{eq}}\right) \\ j = i, v; \ k \neq j = i, v, \end{gathered} \tag{10}$$

where traps occupation probabilities are obtained by solving the following steady-state balance equations [50]:

$$\begin{aligned} &\left(1 - f_j\right)K_j\left(C_j - C_j^{\mathrm{eq}}\right) - zf_jK_k\left(C_k - C_k^{\mathrm{eq}}\right) - \alpha_s f_j f_k \\ &\quad = 0 \quad j = i, v; \ k \neq j = i, v. \end{aligned} \tag{11}$$

The parameter α_s is the surface recombination coefficient that depends on the specific features of interfaces structure, such as the distance between trapping sites and their energy. It may be assumed that all the interface characteristics that affect point defect absorption or annihilation may be lumped in this parameter. Factor z represents the number of different jumps to a site by which recombination can occur [50]. In this work, it is set to be equal to 4 for any material structure. In this way, the model gives the highest importance to the effect of the recombination between trapped point defects with respect to the recombination between a trapped point defect and a point defect jumping into the interface from the matrix (cf. (11)). Further details about this choice will be given in Section 3.

The model consisting of the balance equations (1) along with their initial conditions, (2), and their boundary conditions, that is, (7), in the case of interfaces acting as neutral sinks, or (10), in the case of interfaces acting as variable-biased sinks, allows one to describe the temporal evolution of point defect concentrations inside a single layer of a given material undergoing radiation.

A change of variables was used in this work in order to obtain dimensionless and normalized equations and parameters. This may help in analyzing the behavior of the system for different values of the parameters because this strategy typically reduces the number of parameters. Following the approach of Krantz [51], it is possible to define the dimensionless point defect concentrations as

$$C_j^* = \frac{C_j - C_j^{(r)}}{C_j^{(s)}} \quad j = i, v, \tag{12}$$

where superscripts r and s represent the reference and the scaling value, respectively. Accordingly, the dimensionless spatial coordinate and time may be defined as follows:

$$x^* = \frac{x - x^{(r)}}{x^{(s)}}, \tag{13}$$

$$t^* = \frac{t - t^{(r)}}{t^{(s)}}. \tag{14}$$

Let us now assume for the reference and scaling variables the following expressions:

$$C_j^{(r)} = C_j^{\text{eq}} \quad j = i, v, \tag{15}$$

$$C_j^{(s)} = \sqrt{\frac{K^0}{K_{iv}}} \quad j = i, v, \tag{16}$$

$$x^{(r)} = 0, \tag{17}$$

$$x^{(s)} = L, \tag{18}$$

$$t^{(r)} = 0, \tag{19}$$

$$t^{(s)} = \frac{L^2}{D_i}. \tag{20}$$

It may be worth noting that $t^{(s)}$ can be also regarded as the characteristic time of interstitials diffusion along the metal layer.

According to this change of variables, the evolution of point defects dimensionless concentrations as a function of the dimensionless time is described by the dimensionless equation,

$$\frac{\partial C_j^*}{\partial t^*} - D_j^* \frac{\partial^2 C_j^*}{\partial x^{*2}} = A\left(1 - C_i^* C_v^*\right) \quad j = i, v, \tag{21}$$

along with the initial conditions

$$\begin{aligned} t^* &= 0, \quad \forall x^* \\ C_j^* &= 0 \quad j = i, v. \end{aligned} \tag{22}$$

The dimensionless diffusion coefficient D_j^* is defined with respect to the diffusion coefficient of SIAs:

$$D_j^* = \frac{D_j}{D_i} \quad j = i, v. \tag{23}$$

Consequently, the dimensionless diffusion coefficient for interstitials is equal to 1, while the dimensionless diffusion coefficient for vacancies is typically much smaller than 1, as the diffusion of interstitials is significantly faster than the diffusion of vacancies. The dimensionless parameter A is expressed as

$$A = \sqrt{\frac{L^4 K^0 \alpha_{iv} \Omega}{a^2} \frac{\left(D_i + D_v\right)}{D_i^2}} \tag{24}$$

and it represents the ratio between the characteristic times of point defect recombination and production phenomena.

Dimensionless boundary conditions for the case of neutral sinks are expressed as

$$\begin{aligned} x^* &= 0; \quad x^* = 1 \quad \forall t^* \\ D_j^* \frac{\partial C_j^*}{\partial x^*} &= \frac{D_j^*}{b^*} C_j^* \quad j = i, v, \end{aligned} \tag{25}$$

where the dimensionless parameter b^* is defined as

$$b^* = \frac{b}{L}. \tag{26}$$

In the case of interfaces acting as variable-biased sinks, the boundary conditions may be expressed as

$$\begin{aligned} x^* &= 0; \quad x^* = 1 \quad \forall t^* \\ D_j^* \frac{\partial C_j^*}{\partial x^*} &= \left(1 - f_j + z f_k\right) \frac{D_j^*}{b^*} C_j^* \\ & \qquad j = i, v; \ k \neq j = i, v. \end{aligned} \tag{27}$$

The dimensionless steady-state balance equations of occupation probabilities appear as follows:

$$\begin{aligned} \left(1 - f_j\right) D_j^* C_j^* - z f_j D_k^* C_k^* - E f_j f_k = 0 \\ j = i, v; \ k \neq j = i, v, \end{aligned} \tag{28}$$

where the dimensionless parameter E is defined as

$$E = \sqrt{\frac{b^2 \alpha_s^2 \alpha_{iv} \Omega}{K^0 a^2} \frac{\left(D_i + D_v\right)}{D_i^2}} \tag{29}$$

and expresses the ratio between the characteristic times of point defect annihilation at interfaces and net production phenomena.

With the aim of better evaluating metallic multilayers performances in terms of radiation resistance the following definition of efficiency is introduced in this work:

$$\eta_j = 1 - \frac{C_j - C_j^{(\min)}}{C_j^{(\max)} - C_j^{(\min)}} \quad j = i, v. \tag{30}$$

It may be regarded as the efficiency of multilayers for j-type point defects absorption or removal. The limiting concentrations $C_j^{(\min)}$ and $C_j^{(\max)}$ represent the minimum and maximum point defects concentrations achievable in metallic layers during irradiation, respectively.

While the minimum concentration $C_j^{(\min)}$ may be easily identified as the equilibrium concentration C_j^{eq} consistently with (15), the maximum concentration deserves additional comments. Specifically, it may be thought of as the point defect concentration achieved under the particular condition of absence of sinks for point defects. With the aim of better clarifying this important point, let us consider a single layer of thickness L bounded by two interfaces unable to absorb defects. Equations (1) still represent the balance equations for point defects within the layer. However, the coupled boundary conditions should be now expressed as insulated ones:

$$\begin{aligned} x &= 0; \quad x = L, \quad \forall t \\ \frac{\partial C_j}{\partial x} &= 0 \quad j = i, v. \end{aligned} \tag{31}$$

Numerical solution of (1) along with boundary condition (31) showed that the maximum achievable point defect concentration resembles the stationary state one. In particular, it may be easily found that

$$C_j^{(\max)} = C_j^{\mathrm{eq}} + \sqrt{\frac{K^0}{K_{iv}}} \quad j = i, v, \tag{32}$$

which expresses the equilibrium between the recombination rate and the production rate. It may be easily recognized that the difference between maximum and minimum concentrations represents the scaling concentration introduced by (16), which is time-independent and assumes the same value for both vacancies and SIAs. It is worth noting that, according to its definition, efficiency measures the additional contribution of interfaces to point defect annihilation being the base case represented by the contribution of volumetric recombination only.

Eventually, according to the nondimensionalizing procedure, the efficiency of interfaces for point defects absorption may be also expressed as

$$\eta_j = 1 - C_j^* \quad j = i, v. \tag{33}$$

The nondimensional model obtained through this change of variables has only four dimensionless parameters: A, D_v^*, b^*, and E. This model has been solved for a wide range of values of all the dimensionless parameters, paying attention to keeping their physical meaning.

The equations of the dimensionless model were solved numerically as a time-dependent problem. In the case of interfaces acting like variable-biased sinks, the system of equations consists of coupled algebraic and differential equations. The model was solved through Comsol Multiphysics using the diffusion and convection module and the ODE and DAE interfaces. The parameter dependences were studied through the parametric sweep extension step. The model parameters were those pertaining to copper and niobium and their values are reported in Tables 1 and 2, respectively.

3. Results and Discussion

In the following, the behavior of a single layer with isolated (nonabsorbing) interfaces undergoing irradiation represents the base case to which the effect of interfaces is compared when they are modelled as neutral (perfect) sinks and variable-biased sinks. The same reference allows evaluating removal efficiency of point defects as function of the relevant variables and mapping out layers performance in terms of dimensionless parameters. Results are obtained solving the dimensionless version of the model. Accordingly, outputs are shown as a function of dimensionless variables. On the other hand, interpretation of results is reported with reference to geometric and operating conditions such as layer thickness, temperature, and irradiation conditions. This way model results are better related to practical applications of multilayers in nuclear field.

Table 1: Model parameters for copper.

Parameters	Unit	Value	Reference
a	m	3.6147×10^{-10}	—
b	m	2.556×10^{-10}	—
E_i^F	J	4.3739×10^{-19}	[52]
E_v^F	J	2.0348×10^{-19}	[49]
E_i^M	J	0.1314×10^{-19}	[52]
E_v^F	J	1.2817×10^{-19}	[49]
k_B	$\mathrm{J\,K^{-1}}$	$1.3806488 \times 10^{-23}$	—
K^0	$\mathrm{m^{-3}\,s^{-1}}$	10^{20}	This work
L	m	10^{-9}–10^{0}	This work
S_i^F	$\mathrm{J\,K^{-1}}$	0	[49]
S_v^F	$\mathrm{J\,K^{-1}}$	$3.31356072 \times 10^{-23}$	[49]
S_i^M	$\mathrm{J\,K^{-1}}$	0	[49]
S_v^M	$\mathrm{J\,K^{-1}}$	0	[49]
S_j^{tot}	$\mathrm{m^{-2}}$	2.0×10^{17}	This work
T	K	573.15–973.15	This work
z	—	4	This work
α_i	—	0.5	[49]
α_{iv}	—	48	[49]
α_s	$\mathrm{m^{-2}\,s^{-1}}$	0–10^{30}	This work
α_v	—	1	[49]
ν_D	$\mathrm{s^{-1}}$	10^{13}	[49]
Ω	$\mathrm{m^3}$	1.182×10^{-29}	—

Table 2: Model parameters for niobium.

Parameters	Unit	Value	Reference
a	m	3.303×10^{-10}	—
b	m	2.86×10^{-10}	—
E_i^F	J	7.386×10^{-19}	[53]
E_v^F	J	4.442×10^{-19}	[53]
E_i^M	J	0.128174×10^{-19}	[54]
E_v^F	J	1.0254×10^{-19}	[53]
k_B	$\mathrm{J\,K^{-1}}$	$1.3806488 \times 10^{-23}$	—
K^0	$\mathrm{m^{-3}\,s^{-1}}$	10^{20}	This work
L	m	10^{-9}–10^{0}	This work
S_i^F	$\mathrm{J\,K^{-1}}$	0	This work
S_v^F	$\mathrm{J\,K^{-1}}$	$2.8993625 \times 10^{-23}$	[55]
S_i^M	$\mathrm{J\,K^{-1}}$	0	This work
S_v^M	$\mathrm{J\,K^{-1}}$	$0.9964542 \times 10^{-23}$	[55]
S_j^{tot}	$\mathrm{m^{-2}}$	2.0×10^{17}	This work
T	K	573.15–773.15	This work
z	—	4	This work
α_i	—	0.16	[49]
α_{iv}	—	36	This work
α_s	$\mathrm{m^{-2}\,s^{-1}}$	0–10^{30}	This work
α_v	—	1	[49]
ν_D	$\mathrm{s^{-1}}$	10^{13}	[49]
Ω	$\mathrm{m^3}$	1.8×10^{-29}	—

3.1. Interfaces as Perfect Sinks. A single 100 nm thick layer of copper undergoing radiation with a defect production rate

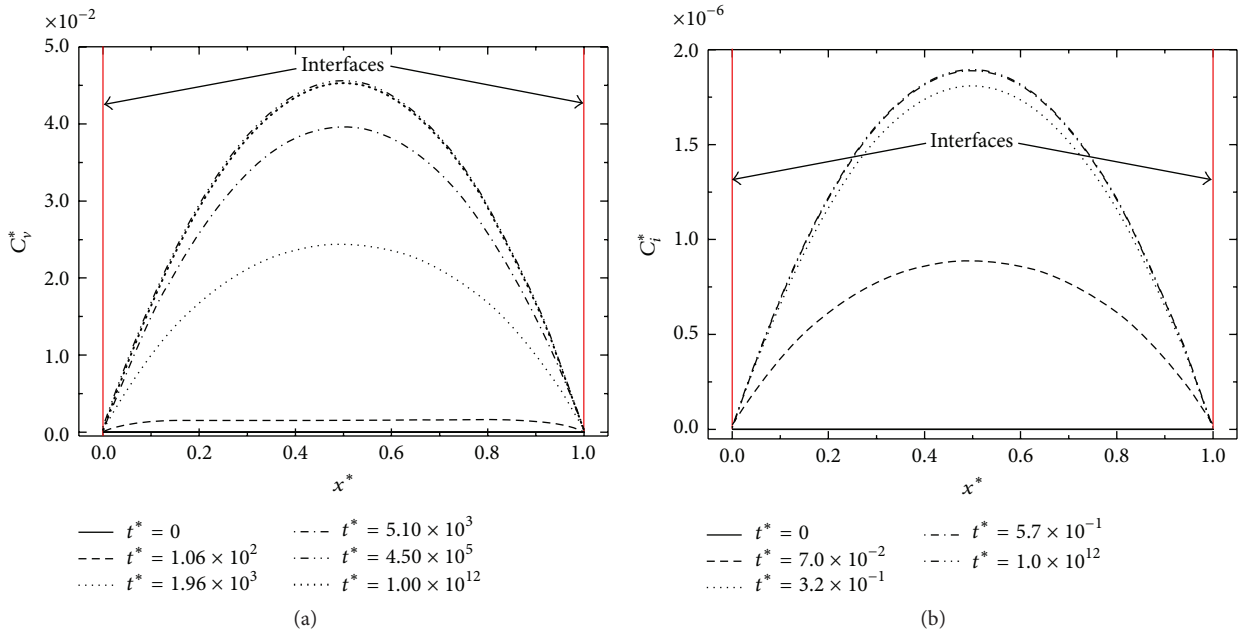

Figure 1: Spatial profiles of (a) vacancy and (b) SIA concentrations in a single layer of copper bounded by two interfaces acting as neutral sinks at different dimensionless times ($T = 773.15$ K; $L = 1 \times 10^{-7}$ m; $K^0 = 1 \times 10^{20}$ m^{-3} s^{-1}).

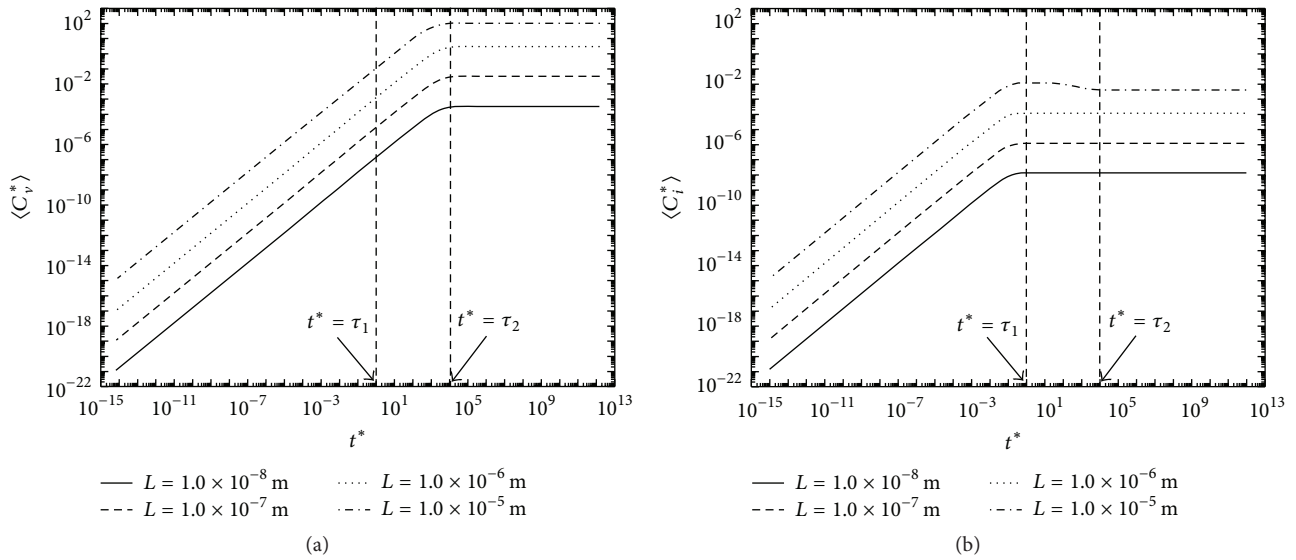

Figure 2: Temporal profiles of average (a) vacancy and (b) SIA concentrations in a single layer of copper of different thicknesses L bounded by two interfaces acting as neutral sinks ($T = 773.15$ K; $K^0 = 1 \times 10^{20}$ m^{-3} s^{-1}).

$K^0 = 10^{20}$ m^{-3} s^{-1} at the temperature $T = 773.15$ K is taken into account as a base case. The interfaces are assumed to behave as perfect sinks, and (9) is adopted as boundary conditions. Spatial profiles of vacancy and SIA concentration are shown in Figure 1 at different dimensionless times. Besides the expected parabolic profile, it is easy to notice that the initial concentrations increase according to the production of point defects by irradiation. Indeed, at the beginning, the concentrations are too low for either volume or interface recombination to have an effect on the build-up. Then, when the production rate is compensated by the recombination rate, point defects concentrations will start to level off and spatial profiles become time invariant; that is, a stationary state is reached. It may clearly be seen that concentrations at interfaces remain constant according to (9).

The dimensionless average concentrations of vacancies and SIAs defined as

$$\left\langle C_j^* \right\rangle = \frac{\int_0^1 C_j^*(x^*)\, dx^*}{\int_0^1 dx^*} \quad j = i, v \tag{34}$$

are reported in Figure 2. Results are shown in a double-log plot versus dimensionless time for different layer thicknesses

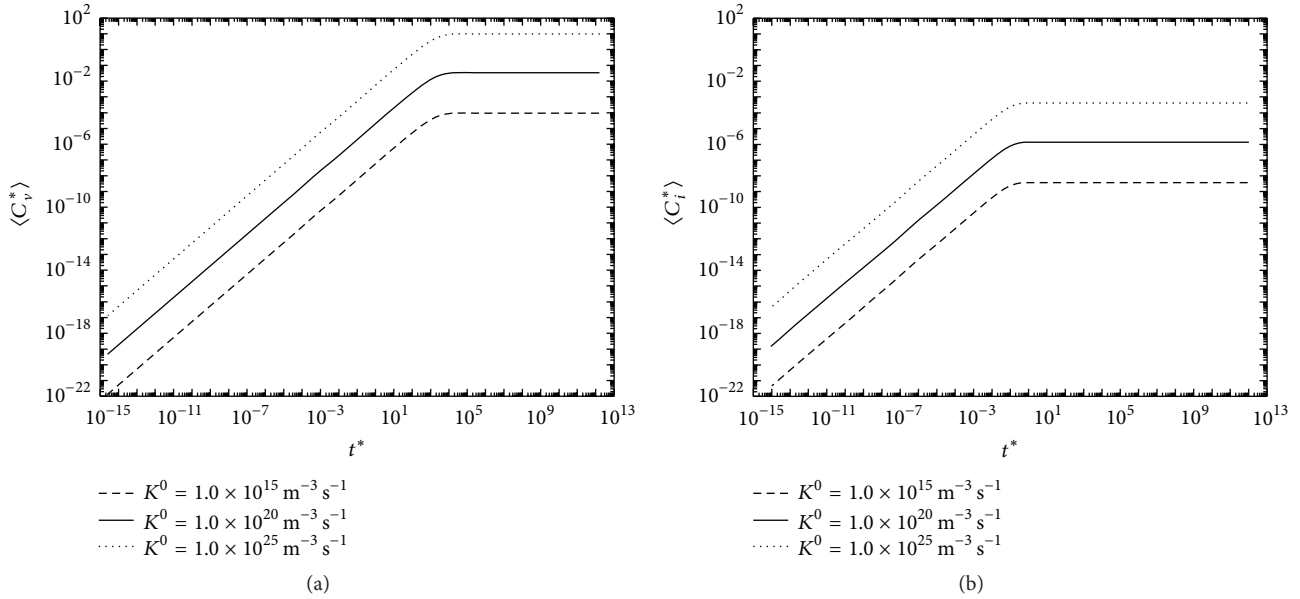

Figure 3: Temporal profiles of average (a) vacancy and (b) SIA concentrations in a single layer of copper bounded by two interfaces acting as neutral sinks undergoing irradiation with different production rates of point defects ($T = 773.15$ K; $L = 1 \times 10^{-7}$ m).

of a single copper layer ($K^0 = 10^{20}\ \mathrm{m^{-3}\,s^{-1}}$; $T = 773.15$ K). By comparing Figures 2(a) and 2(b), it may be seen that average SIA concentration always reaches the steady state at the characteristic time τ_1, while average vacancies concentration profile becomes time-invariant at the characteristic time $\tau_2 > \tau_1$. It might be worth noting that SIAs concentration reaches the stationary state before vacancies' one because $D_i > D_v$, which implies that interstitials reach interfaces faster than vacancies causing a higher annihilation rate of the former.

As a general result, it can be seen that the steady-state point defect concentrations increase as layer thickness increases. This is due to increasing length of the diffusion path, which reduces the additional contribution of point defect annihilation at interfaces. Indeed, at a very large layer thickness, the only effective phenomenon of point defect removal is the volume recombination and model results approach the ideal case of isolated interfaces: $\langle C_j^* \rangle = 1$, $j = i, v$.

A peculiar behavior of the system for large layer thickness is worth noting. In this case, depending on the layer thickness, it may happen that the steady-state average concentration of SIAs results to be lower than the one corresponding to the ideal case of isolated interfaces, that is, $\langle C_i^* \rangle = 1$, while the average concentration of vacancies results to be simultaneously higher, that is, $\langle C_v^* \rangle$ greater than unity. In this case, in a paradoxical way, the presence of interfaces capable of absorbing defects makes the layer performance worsen. Referring to the results reported in Figure 2(a), it appears that presence of absorbing interfaces in a single layer undergoing irradiation enhances the removal of vacancies only if the thickness is equal to or smaller than 100 nm. On the contrary, absorbing interfaces in thicker layers cause an average vacancy concentration higher than the case of nonabsorbing (i.e., isolated) interfaces. The reason of this behavior may be explained considering the different diffusivity of interstitials and vacancies. Indeed, since vacancy and SIA concentrations do not have the same dynamic behavior, interstitials reach interfaces where they are annihilated, while vacancies remain in the layer bulk without the possibility to efficiently recombine due to the decreasing interstitials concentration.

The effects of defect production rates K^0 on the dimensionless average concentrations of vacancies and SIAs are reported in Figure 3 in a double-log plot versus dimensionless time for a single layer of copper of 100 nm thickness, undergoing radiation at the temperature $T = 773.15$ K. The defect production rate does not affect the characteristic times for the onset of steady state in both vacancy and SIA concentration profiles. However, the defect point steady-state concentrations increase as K^0 increases. For instance, the presence of interfaces in a single layer of 100 nm results to be ineffective in vacancies removing for a defect production rate of $10^{25}\ \mathrm{m^{-3}\,s^{-1}}$; that is, $\langle C_v^* \rangle$ at steady state is higher than unity (cf. Figure 3(a)).

Figure 4 shows the dimensionless average concentrations of vacancies and SIAs in a double-log plot versus dimensionless time for a single 100 nm thick layer of copper irradiated with the defect production $K^0 = 10^{20}\ \mathrm{m^{-3}\,s^{-1}}$ at different temperatures. Temperature does not noticeably affect the SIA steady state concentration in the range investigated, that is, 300–700 K. On the contrary, characteristic time of vacancies annihilation at the interfaces decreases as temperature increases and the steady-state vacancy average concentration reduces too. It can be seen that at the lowest temperature investigated interfaces result to be ineffective in vacancy removal.

According to the results presented so far, the ability of a single layer of copper bounded by interfaces which behave as

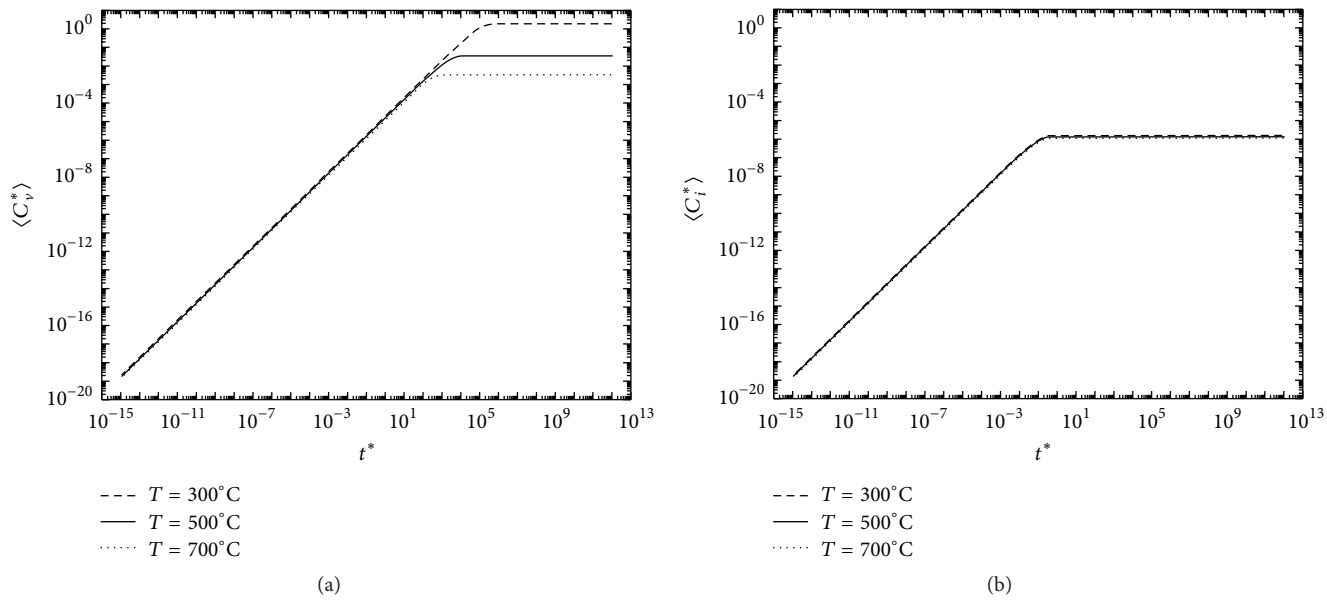

Figure 4: Temporal profiles of average (a) vacancy and (b) SIA concentrations in a single layer of copper bounded by two interfaces acting as neutral sinks undergoing irradiation at different temperatures ($L = 1 \times 10^{-7}$ m; $K^0 = 1 \times 10^{20}$ m^{-3} s^{-1}).

neutral sinks to remove radiation-induced defect is affected by layer thickness, as well as defect production rate and temperature. Moreover, concentrations of interstitials and vacancies show a significantly different behavior. This finding may be explained by the diverse diffusion rate of interstitials and vacancies.

3.2. Interfaces as Variable-Biased Sinks. In order to generalize this study, the model is also solved assuming the interfaces behaving like variable-biased sinks. Then, (10) is adopted as boundary conditions of (1). The most important parameter of this mathematical description is the surface recombination coefficient α_s. As already stated, it lumps the specific interface features affecting interaction with point defects. Unfortunately, it may be difficult to *a priori* evaluate. Therefore, it is taken as an unknown parameter of the model and a parametric sensitivity is performed to evaluate the effect of α_s on model outputs.

Temporal profiles of the average concentrations of vacancies and SIAs as well as occupation probabilities of traps of vacancies and SIAs are reported in Figure 5 for different values of the surface recombination coefficient. When the surface recombination coefficient α_s is nil, occupation probability of each of defect traps continuously increases with time (cf. Figure 5(a)), although more slowly while approaching steady state. As the parameter α_s increases, f_v first increases, then it starts to decrease, and finally it reaches a steady state. It can be seen that steady-state occupational probability of vacancy traps decreases as α_s increases. The occupational probability of interstitial traps is shown in Figure 5(b). At relatively low values of the parameter α_s, f_i steady-state value decreases as α_s increases. However, f_i profile becomes invariant as the surface recombination coefficient increases. Looking at the equation describing the occupation probabilities, it can be inferred that the dissimilar behavior of interfaces for interstitials and vacancies is likely due to the different diffusivity of the defects.

On the other hand, according to mathematical description of Brailsford and Bullough [50] the specific interface structure, whose features are lumped in the recombination coefficient, results not to affect the average point defect concentrations. Indeed, it is evident in Figures 5(c) and 5(d) that average concentrations profiles of point defects are invariant with respect to the parameter α_s. Thus, it may be concluded that the recombination between a trapped point defect and a point defect jumping into the interface from the matrix is the only effective mechanism of defect annihilation at the interfaces (cf. (28)). Since the model overestimates the effect of recombination between trapped point defects with respect to recombination between a trapped point defect and a point defect jumping into the interface from the matrix, as already discussed in Section 2, the first one results to be unquestionably negligible. Moreover, at the considered operating conditions (i.e., 100 nm thickness, defect production rate of 10^{20} m^{-3} s^{-1}, and 500°C) the temporal profiles of the average concentrations of vacancies and SIAs do not change whether interfaces act as neutral or variable-biased sinks (see comparison between Figures 2, 5(c), and 5(d)). The same result was obtained when varying the operating conditions (not shown). In other words, it can be concluded that interfaces of copper layers catalyze the point defect annihilation reaction acting as perfect sinks whatever their structure/nature. These model results are in agreement with experimental ones of Mao et al. [22] who observed that Cu-Nb interfaces behave like perfect sinks for vacancies in copper.

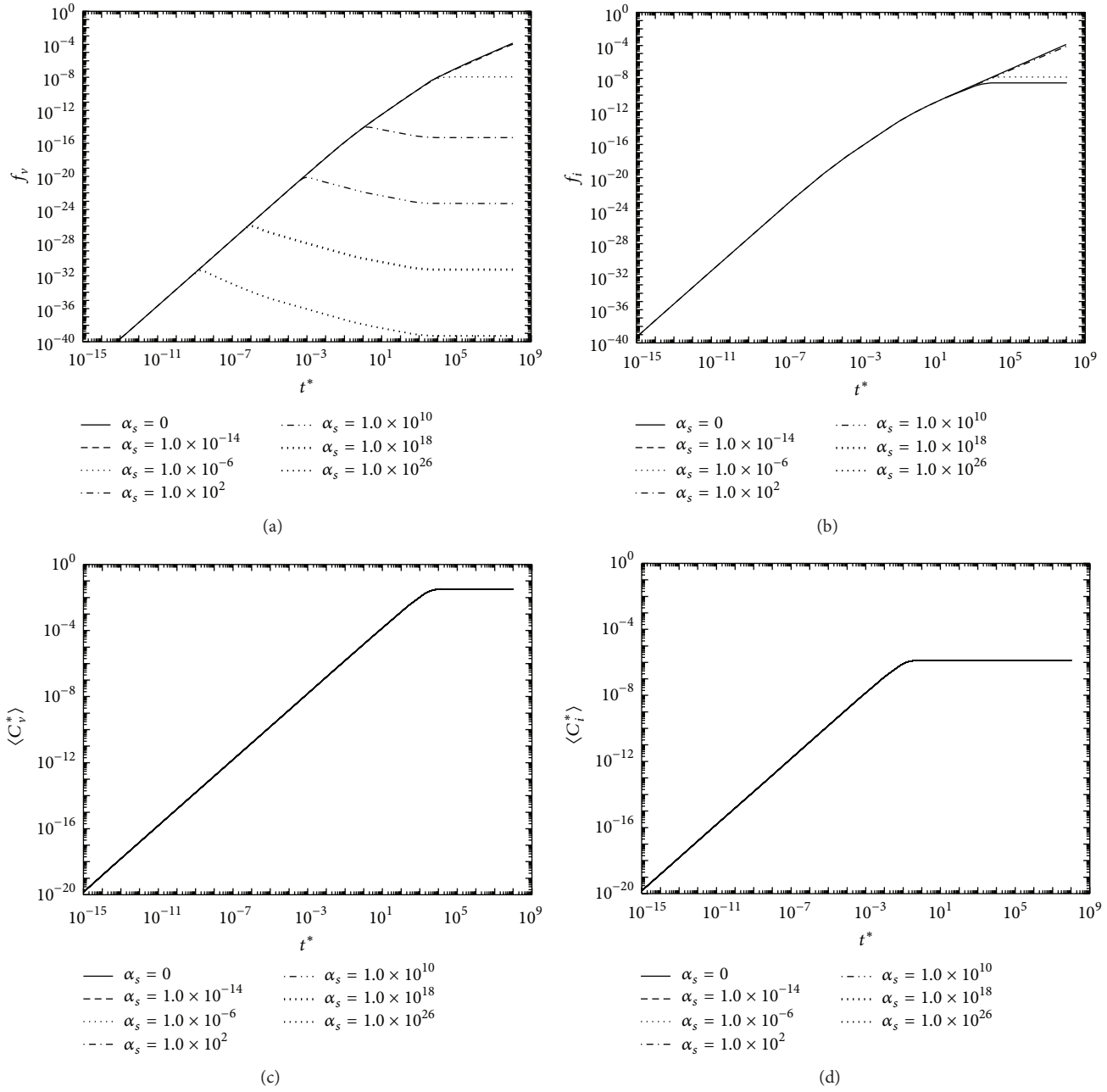

FIGURE 5: Temporal profiles of occupation probability of (a) vacancy and (b) SIA traps, and average concentrations of (c) vacancies and (d) SIAs in a single layer of copper bounded by two interfaces acting as variable-biased sinks for different values of the surface recombination coefficient, α_s ($T = 773.15$ K; $L = 1 \times 10^{-7}$ m; $K^0 = 1 \times 10^{20}$ m^{-3} s^{-1}).

3.3. Comparison between Copper and Niobium Layers. As already pointed out in Section 1, Cu-Nb interfaces have been found to be highly stable under radiation and, for this reason, they are largely studied in the literature. In this work, the effect of interfaces also in single Nb layers is studied for the sake of completeness. With the aim of congruently comparing copper and niobium layers, the point defect production rate in the latter ones is calculated through the SRIM software program. In particular, it has been found that the radiation generating a defect production rate of 10^{20} m^{-3} s^{-1} in copper layers produces point defects at the rate of 5×10^{20} m^{-3} s^{-1} in layers of niobium.

Temporal profiles of the average vacancy and SIA concentrations in a 100 nm thick single layer of copper and niobium undergoing irradiation with a production rate of 10^{20} m^{-3} s^{-1} and 5×10^{20} m^{-3} s^{-1}, respectively, are compared in Figure 6. It may be clearly seen that time for the vacancy steady-state achievement is smaller for niobium than for copper (cf. Figure 6(a)). This result is likely due to the higher vacancy diffusion coefficient in niobium. Moreover,

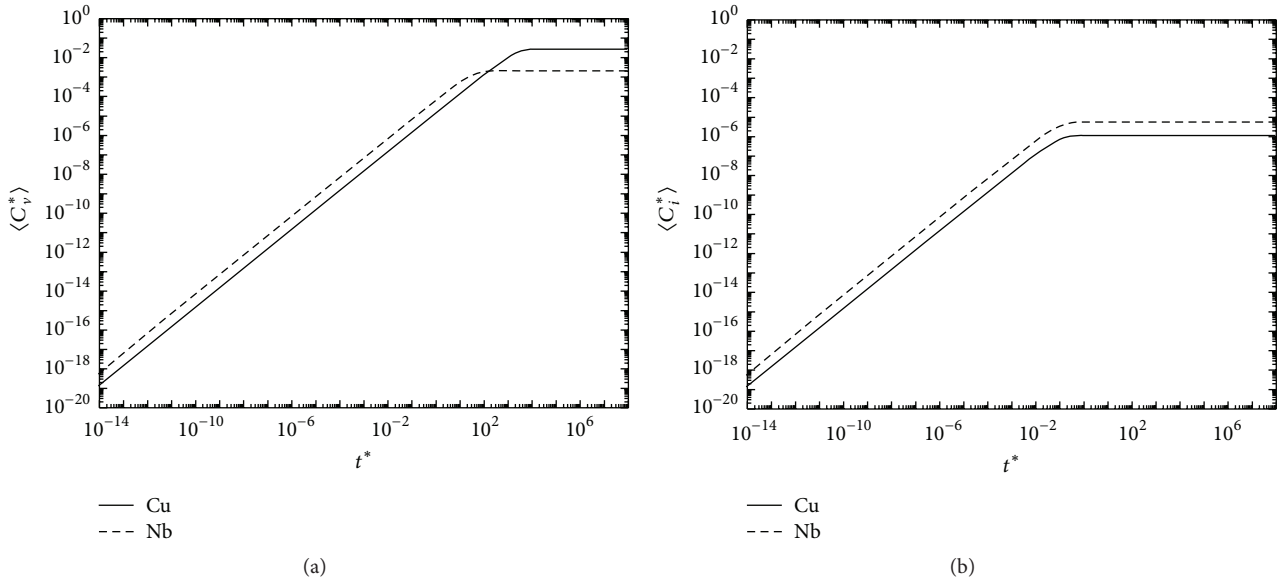

FIGURE 6: Temporal profiles of the average (a) vacancy and (b) SIA concentrations in a single layer of copper and niobium bounded by two interfaces as neutral sinks ($T = 773.15$ K; $L = 1 \times 10^{-7}$ m; $K^0 = 1 \times 10^{20}$ m^{-3} s^{-1}).

the steady-state concentration of vacancies is quite lower in a layer of niobium. On the contrary, the steady-state concentration of interstitials is lower in layers of copper, while interstitial concentration steady-state achievement is almost the same for both metals (cf. Figure 6(b)). The effects of layer thickness, point defects production rate, and temperature on average point defects concentrations are basically the same for both copper and niobium (not shown). Moreover, model simulations of niobium layers predict identical behavior for both cases of interface acting as neutral or variable-biased sinks.

3.4. Removal Efficiency of Point Defects. In order to verify the effect of interfaces features in a wide range of system conditions, the model was solved for different layer thickness assuming interfaces acting as neutral or variable-biased sinks for both copper and niobium. The results of these simulations are reported in Figure 7 in terms of point defects absorption (removal) efficiency, with the latter being defined according to (30). Interfaces efficiencies for interstitial removal as a function of thickness in a single layer of copper and niobium are reported in Figures 7(a) and 7(b), respectively. It may be clearly seen that nature of interfaces does not affect the removal efficiency of small thickness layers in both cases. On the contrary, significant differences arise for large thicknesses. Indeed, efficiency for interstitial removal keeps being almost unitary when assuming that interfaces are neutral sink, while it goes down to zero if interfaces are variable-biased sinks. This happens because if interfaces are variable-biased sinks the only effective mechanism of recombination is that between a trapped point defect (typically interstitials) and a point defect jumping into the interface from the matrix (typically vacancies). However, while interstitials reach interfaces very quickly, vacancies struggle to reach interfaces from the bulk in layers of large thickness. This fact gives rise to the low interstitials removal efficiency that characterize thicker layers. It can be although seen that high efficiency of interstitial efficiency is shown by layers of up to about 0.01 m thickness.

Efficiency for vacancies removal is shown in Figures 7(c) and 7(e) for copper and in Figures 7(d) and 7(f) for niobium. Efficiency presents very high value (close to unity) in layers of small thickness (up to about to the order of 10^{-7} m). Then efficiency rapidly goes down to zero as the layer thickness increases, and it reaches negative values for larger thicknesses. Negative efficiency for vacancy removal can be explained as follows. Interfaces remove interstitials faster than vacancies. Therefore, as the efficiency for the interstitial removal increases, a larger quantity of vacancies cannot be removed by volume recombination and therefore accumulates. This means that presence of interfaces promotes the accumulation of vacancies up to reach a steady-state concentration which is higher than that in absence of interfaces. In the case of interfaces as variable-biased sinks this effect partially mitigates for larger thicknesses. Indeed, when the efficiency for interstitial removal decreases as the layer thickness increases, interstitials concentration increases and volume recombination with vacancies can efficiently take place.

Based on the results presented above, it might be concluded that point defect concentrations inside multilayered composite material are primarily affected by layer thickness, while it seems that interface nature (incoherent or semicoherent) plays a significant role only for very large layers. In addition, for each element, it is possible to identify a layer thickness threshold, above which the interfaces become inefficient to remove point defects. This layer thickness threshold depends on the type of point defect considered, as well as on temperature and defect production rate. As an example, Figure 8 shows efficiencies for the vacancy and

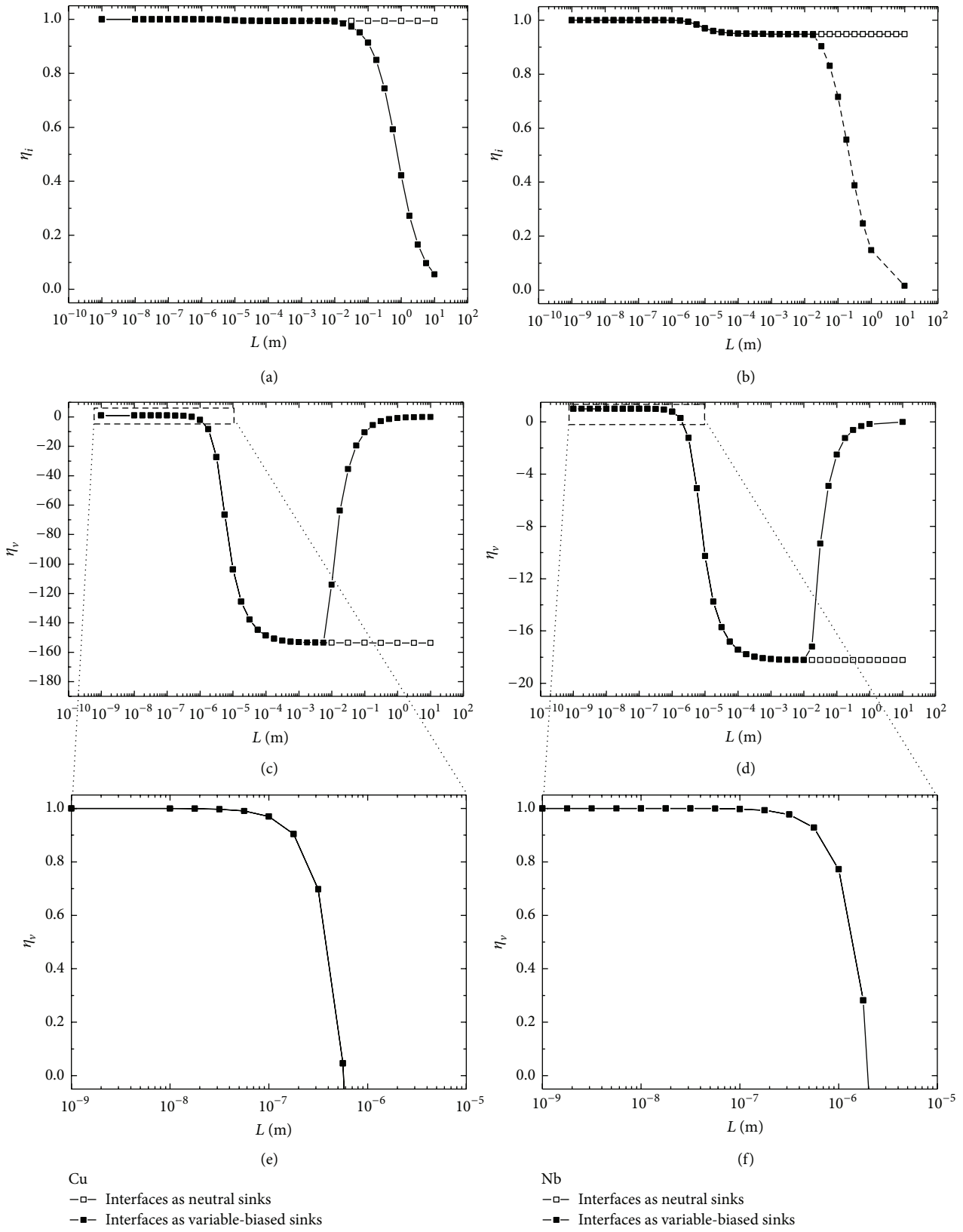

Figure 7: Removal efficiency for SIAs (a-b) and for vacancies (c–f) as functions of the thickness L of a single layer of copper and niobium bounded by interfaces of different type with a surface recombination coefficient α_s nil ($T = 773.15$ K; $K^0 = 1 \times 10^{20}$ m^{-3} s^{-1}).

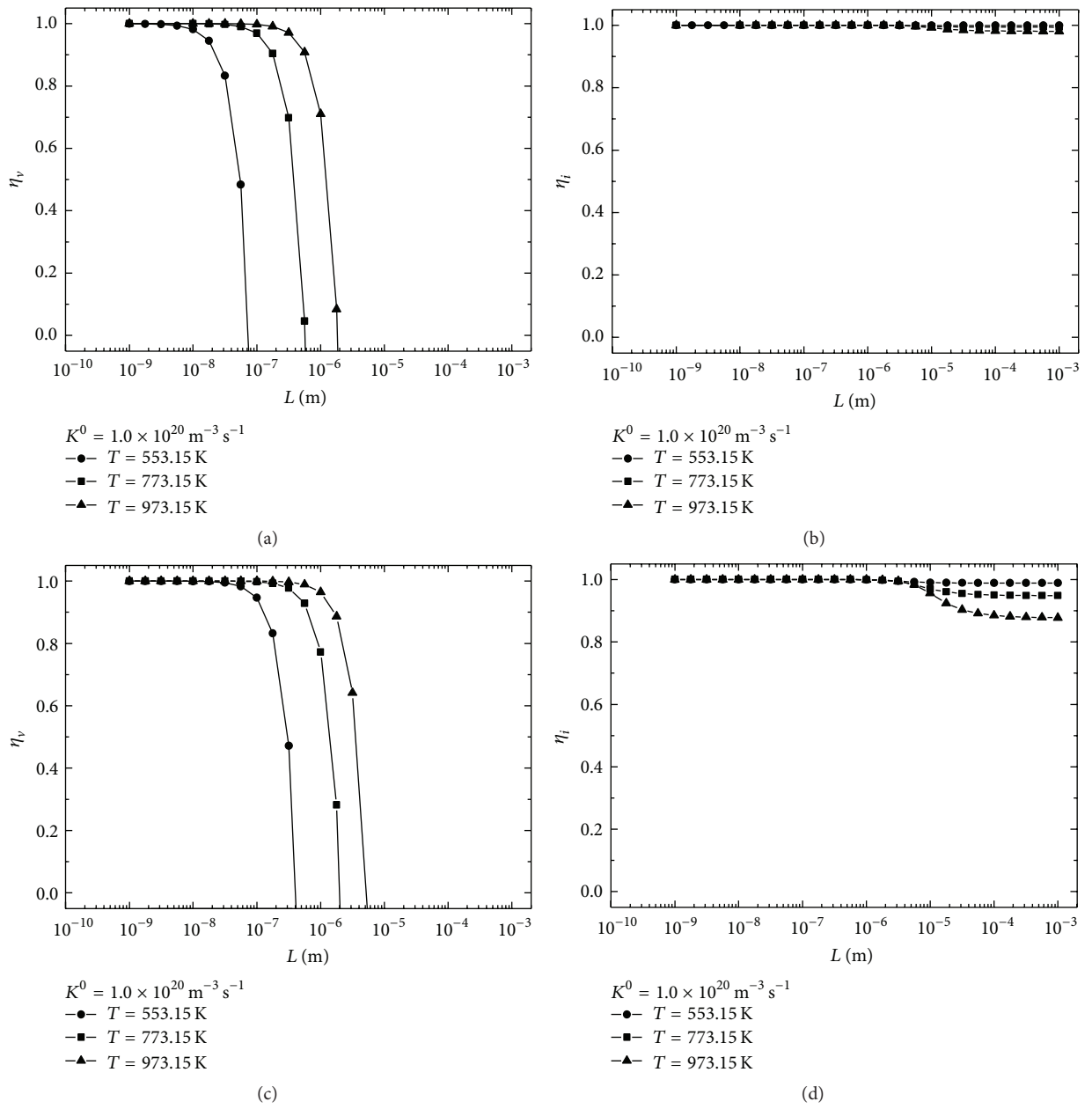

Figure 8: Removal efficiency of point defects as a function of the thickness L of a single layer of copper (a-b) and niobium (c-d) undergoing radiation at different temperatures.

interstitial removal in copper and in niobium as a function of layer thickness at different temperatures. Efficiency of point defect removal starts to decrease at larger thickness as temperature increases. This is because of temperature dependence of point defects diffusivity. Moreover, it may be observed that interstitial efficiency is affected by temperature in lesser degree due to the higher diffusivity of this point defect with respect to vacancies.

Efficiencies for vacancy and interstitial removal in copper and in niobium are reported as a function of the layer thickness for different point defect production rates in Figure 9. As the point defect production rate increases, the efficiency for the removal of vacancies reaches the unitary value at smaller thickness because higher rates of production clearly require higher density of sinks to remove point defects. For instance, at $T = 553.15$ K point defects produced at the rate of 10^{20} m^{-3} s^{-1} in copper and 5×10^{20} m^{-3} s^{-1} in niobium would be theoretically removed with an almost unitary efficiency in a multilayer composite material with 10 nm layers of copper and 100 nm layers of niobium.

It is reported in the literature that advantages for radiation tolerance are not realized until the relevant length scale of multilayers, such as the layer thickness, is reduced to the nanometer range. This result is justified as a consequence of

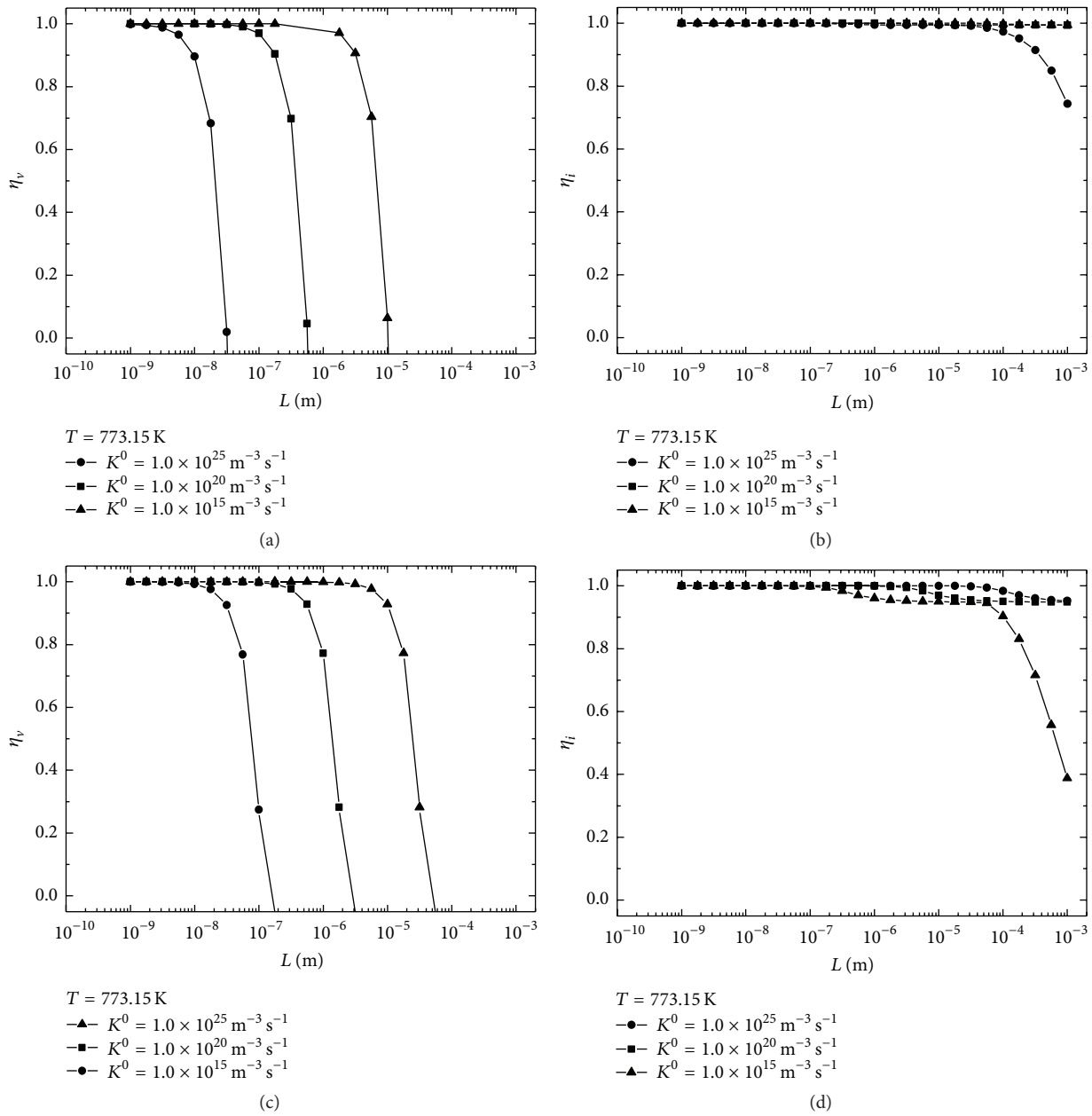

FIGURE 9: Removal efficiency of point defects as a function of the thickness L of a single layer of copper (a-b) and niobium (c-d) undergoing radiation with different production rates of point defects.

short diffusion distance to the nearest sink in such systems. Indeed, in the layered composites of a few nanometers, diffusion distance to sinks is short enough to enable rapid removal of the point defects before they can form into relatively stable aggregates [37]. While the considerations mentioned above qualitatively agree with the results presented in this work, some additional comments are deserved from the quantitative point of view. In fact, model results seem to indicate that the effective layer thickness strongly depends upon radiation conditions and materials involved and that layer thickness should not necessarily be on the order of few nanometers. In addition, it appears that thin layers are needed to remove vacancies, while interstitials are efficiently removed also in thicker layers. These findings form the basis for the need to explore experimentally the stability of layered composite materials over a broad range of irradiation conditions and layer thickness.

3.5. Efficiency Maps. Results shown above clearly indicate that point defect absorption and removal strongly depend on temperature and irradiation conditions. Therefore, materials and thickness should be accurately selected in order to ensure radiation resistance. On the other hand, materials cannot be freely chosen since a couple of immiscible elements are needed in order to guarantee stable interfaces. In addition, even if few nanometers thick layers present very high point

defect removal efficiency, there are doubts that thin layers remain stable under irradiation. For instance, although interfaces in Cu-Nb composites have been proved to be stable, intermixing in Cu-Nb composites may be actually neglected only when considering relatively large thickness layers. Indeed, the lattice results to be really undisturbed at 10–20 nm from the interfaces [22]. Therefore, interfaces of thinner layers would not be stable under irradiation because of the chemical intermixing. On the other hand, if we refer to Figure 8(a), it can be seen that, in order to make a 20 nm thick layer of copper effective, temperature should be increased. Indeed, under the specified radiation conditions, a higher temperature could help remove point defects at the interfaces. However, it is worth noting that temperature cannot be extensively increased in a nuclear reactor.

Therefore, it appears that when designing a multilayer material it is essential to take into account irradiation conditions as well as chemical, physical, and technical constraints. It would be desirable to have different efficient alternatives and select the most suitable one depending upon the technical constraints at hand. The system behavior depends on a large number of parameters. Thus, identification of all possible combinations and classification of them in terms of efficiency performances might result to be cumbersome and time-consuming. In this regard, the dimensionless modelling approach developed in this work may be helpful to reduce complexity and difficulties of the task.

Specifically, multilayers performances in terms of point defects removal can be mapped out in terms of only two dimensionless parameters, named A and D_v^*. As an example, vacancy removal efficiency map is reported in Figure 10, where contour lines for $\eta_v = 0$ and for $\eta_v = 1$ are reported as a function of the two dimensionless parameters mentioned above. These lines define three different areas, where the removal efficiency is almost unitary (white area), where the removal efficiency falls from one to zero (light grey area), and where it is negative (grey area). The main feature of this map is that it is invariant with respect to the other dimensionless model parameters, E and b^*, which have to be taken into account when considering interfaces behaving as variable-biased sinks. Similar map and considerations can be applied to the interstitial removal efficiency.

The map reported in Figure 10 can be easily utilized to predict or estimate vacancy or interstitial removal efficiencies of systems of interest. Indeed, given radiation conditions in terms of point defect production rate and temperature, and selected layer thickness and element made of, the representative point of the system under investigation can be identified by calculating only the two dimensionless parameters mentioned above. As an example of this approach, Figure 10 shows in the vacancy removal efficiency map also some points corresponding to different radiation conditions and thicknesses of copper and niobium layers. A set of system conditions where layered materials theoretically exhibit radiation resistance is easily recognized as falling in the white area.

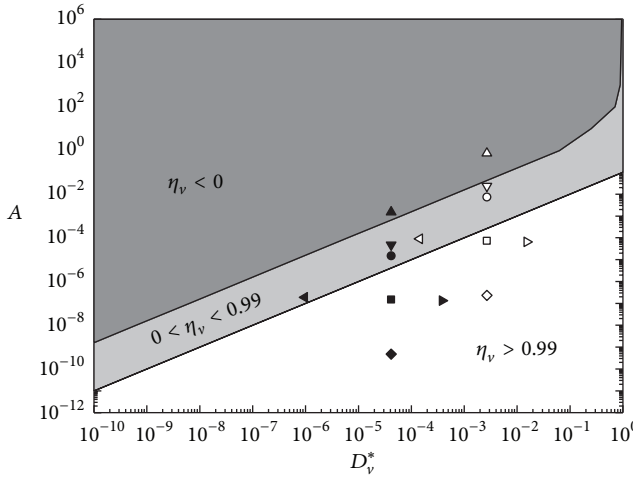

- $T = 500^\circ\text{C}$; $K^0 = 10^{20}\ \text{m}^{-3}\ \text{s}^{-1}$; $L = 10^{-8}$ m
- $T = 500^\circ\text{C}$; $K^0 = 10^{20}\ \text{m}^{-3}\ \text{s}^{-1}$; $L = 10^{-7}$ m
- $T = 500^\circ\text{C}$; $K^0 = 10^{20}\ \text{m}^{-3}\ \text{s}^{-1}$; $L = 10^{-6}$ m
- $T = 500^\circ\text{C}$; $K^0 = 10^{25}\ \text{m}^{-3}\ \text{s}^{-1}$; $L = 10^{-8}$ m
- $T = 500^\circ\text{C}$; $K^0 = 10^{15}\ \text{m}^{-3}\ \text{s}^{-1}$; $L = 10^{-8}$ m
- $T = 300^\circ\text{C}$; $K^0 = 10^{20}\ \text{m}^{-3}\ \text{s}^{-1}$; $L = 10^{-8}$ m
- $T = 700^\circ\text{C}$; $K^0 = 10^{20}\ \text{m}^{-3}\ \text{s}^{-1}$; $L = 10^{-8}$ m
- $T = 500^\circ\text{C}$; $K^0 = 5 \times 10^{20}\ \text{m}^{-3}\ \text{s}^{-1}$; $L = 10^{-7}$ m
- $T = 500^\circ\text{C}$; $K^0 = 5 \times 10^{20}\ \text{m}^{-3}\ \text{s}^{-1}$; $L = 10^{-6}$ m
- $T = 500^\circ\text{C}$; $K^0 = 5 \times 10^{20}\ \text{m}^{-3}\ \text{s}^{-1}$; $L = 10^{-5}$ m
- $T = 500^\circ\text{C}$; $K^0 = 5 \times 10^{25}\ \text{m}^{-3}\ \text{s}^{-1}$; $L = 10^{-7}$ m
- $T = 500^\circ\text{C}$; $K^0 = 5 \times 10^{15}\ \text{m}^{-3}\ \text{s}^{-1}$; $L = 10^{-7}$ m
- $T = 300^\circ\text{C}$; $K^0 = 5 \times 10^{20}\ \text{m}^{-3}\ \text{s}^{-1}$; $L = 10^{-7}$ m
- $T = 700^\circ\text{C}$; $K^0 = 5 \times 10^{20}\ \text{m}^{-3}\ \text{s}^{-1}$; $L = 10^{-7}$ m

Figure 10: Removal efficiency map in terms of the dimensionless parameters A versus D_v^* and effect of layer thickness L, point defect production rate K^0, and temperature T on removal efficiency for copper (black symbols) and niobium (white symbols).

4. Concluding Remarks

The present work provides a generalized continuum model of the point defects dynamics in nanometer-sized multilayer composites. Numerical findings regarding the Cu/Nb case study indicate that the point defect removal capability of individual Cu and Nb layers terminated by interfaces behaving as neutral sinks is affected by layer thickness, defect production rate, and temperature. Interstitials and vacancies exhibit significantly different behavior due to the different diffusion rates of interstitials and vacancies in bulk materials. To a first approximation, interfaces modelled as variable-biased sinks do not depress average point defect contents. Recombination between point defect trapped at interfaces and incoming point defects represents the only effective point defect annihilation mechanism, being recombination between point defects trapped at interfaces negligible. Cu/Nb interfaces mostly behave as perfect sinks independent of their structure, in agreement with experimental findings demonstrating the tendency of behaving as perfect sinks for Cu vacancies shown by Cu/Nb interfaces. The most effective layer thickness strongly depends on irradiation conditions, and not necessarily it must range on the nanometer scale. In this regard, asymmetry exists between vacancies and interstitials.

Interestingly, the performance of multilayers in terms of point defect removal can be mapped out using two parameters, namely, dimensionless vacancy diffusivity and

the ratio between the characteristic times of point defect recombination and production. In principle, such maps can be used to estimate the efficiency of vacancy and interstitial removal in any given multilayer composite material. Once irradiation conditions are defined in terms of point defect production rate, temperature, and layer thickness, the material behavior can be assessed by calculating only the two mentioned dimensionless parameters.

Nomenclature

a: Lattice constant, m
A: Dimensionless production rate of point defects, —
b: Lattice spacing, m
C: Concentration of point defects, m^{-3}
D: Diffusivity, $m^2\ s^{-1}$
E: Dimensionless surface recombination parameter, —
E^F: Activation energy of formation of point defects, J
E^M: Activation energy of mobility of point defects, J
f: Occupation probability, —
k_B: Boltzmann constant, $J\ K^{-1}$
K: Transfer velocity, —
K_{iv}: Recombination factor of the antidefects, $m^3\ s^{-1}$
K^0: Production rate of point defects, $m^{-3}\ s^{-1}$
L: Domain thickness, m
R^C: Removal rate of point defects due to recombination, $m^{-3}s^{-1}$
S^F: Entropy for formation of point defects, $J\ K^{-1}$
S^M: Entropy for mobility of point defects, $J\ K^{-1}$
T: Temperature, K
t: Time, s
x: Spatial coordinate, m
z: Number of jumps, —.

Greek Letters

α: Diffusion parameter of point defects, —
α_{iv}: Combinatorial factor, —
α_s: Surface recombination coefficient, $m^{-2}\ s^{-1}$
η: Efficiency, —
ν_D: Debye frequency, s^{-1}
Ω: Atomic volume, m^3.

Superscripts

$*$: Dimensionless
(eq): Equilibrium
(max): Maximum
(min): Minimum
(r): Reference
(s): Scaling.

Subscripts

i: Self-interstitial atom
j: Point defect of the type j
v: Vacancy.

Conflict of Interests

The authors declare that there is no conflict of interests regarding the publication of this paper.

Acknowledgment

This work has been supported by the European Community Framework Programme 7, Multiscale Modelling and Materials by Design of Interface-Controlled Radiation Damage in Crystalline Materials (RADINTERFACES) under Grant Agreement no. 263273.

References

[1] M. J. Demkowicz, Y. Q. Wang, R. G. Hoagland, and O. Anderoglu, "Mechanisms of He escape during implantation in CuNb multilayer composites," *Nuclear Instruments and Methods in Physics Research B*, vol. 261, no. 1-2, pp. 524–528, 2007.

[2] S. J. Zinkle and J. T. Busby, "Structural materials for fission & fusion energy," *Materials Today*, vol. 12, no. 11, pp. 12–19, 2009.

[3] W. D. Wilson, C. L. Bisson, and M. I. Baskes, "Self-trapping of helium in metals," *Physical Review B*, vol. 24, no. 10, pp. 5616–5624, 1981.

[4] H. Trinkaus and B. N. Singh, "Helium accumulation in metals during irradiation—where do we stand?" *Journal of Nuclear Materials*, vol. 323, no. 2-3, pp. 229–242, 2003.

[5] R. Escobar Galindo, A. van Veen, J. H. Evans, H. Schut, and J. T. M. De Hosson, "Protrusion formation and surface porosity development on thermally annealed helium implanted copper," *Nuclear Instruments and Methods in Physics Research B*, vol. 217, no. 2, pp. 262–275, 2004.

[6] X. Zhang, N. Li, O. Anderoglu et al., "Nanostructured Cu/Nb multilayers subjected to helium ion-irradiation," *Nuclear Instruments and Methods in Physics Research B*, vol. 261, no. 1-2, pp. 1129–1132, 2007.

[7] K. Hattar, M. J. Demkowicz, A. Misra, I. M. Robertson, and R. G. Hoagland, "Arrest of He bubble growth in Cu-Nb multilayer nanocomposites," *Scripta Materialia*, vol. 58, no. 7, pp. 541–544, 2008.

[8] N. Li, N. A. Mara, Y. Q. Wang, M. Nastasi, and A. Misra, "Compressive flow behavior of Cu thin films and Cu/Nb multilayers containing nanometer-scale helium bubbles," *Scripta Materialia*, vol. 64, no. 10, pp. 974–977, 2011.

[9] M. Samaras, "Multiscale Modelling: the role of helium in iron," *Materials Today*, vol. 12, no. 11, pp. 46–53, 2009.

[10] G. Csiszár, "Evolution of the Burgers-vector population of Cu–Nb multilayers with 7 at% He-implantation determined by X-ray diffraction," *Materials Science and Engineering A*, vol. 609, pp. 185–194, 2014.

[11] A. Misra, M. J. Demkowicz, X. Zhang, and R. G. Hoagland, "The radiation damage tolerance of ultra-high strength nanolayered composites," *JOM: The Journal of the Minerals, Metals & Materials Society*, vol. 59, no. 9, pp. 62–65, 2007.

[12] S. W. Chee, B. Stumphy, N. Q. Vo, R. S. Averback, and P. Bellon, "Dynamic self-organization in Cu alloys under ion irradiation," *Acta Materialia*, vol. 58, no. 12, pp. 4088–4099, 2010.

[13] N. Li, M. Nastasi, and A. Misra, "Defect structures and hardening mechanisms in high dose helium ion implanted Cu and Cu/Nb multilayer thin films," *International Journal of Plasticity*, vol. 32-33, pp. 1–16, 2012.

[14] M. Kaminsky and S. K. Das, "Correlation of blister diameter and blister skin thickness for helium-bombarded V," *Journal of Applied Physics*, vol. 49, no. 11, pp. 5673–5675, 1978.

[15] R. B. Adamson, W. L. Bell, and P. C. Kelly, "Neutron irradiation effects on copper at 327°C," *Journal of Nuclear Materials*, vol. 92, no. 1, pp. 149–154, 1980.

[16] B. Terreault, G. Ross, R. G. St-Jacques, and G. Veilleux, "Evidence that helium irradiation blisters contain high-pressure gas," *Journal of Applied Physics*, vol. 51, no. 3, pp. 1491–1493, 1980.

[17] S. J. Zinkle and K. Farrell, "Void swelling and defect cluster formation in reactor-irradiated copper," *Journal of Nuclear Materials*, vol. 168, no. 3, pp. 262–267, 1989.

[18] J. H. Evans, R. Escobar Galindo, and A. van Veen, "A description of bubble growth and gas release during thermal annealing of helium implanted copper," *Nuclear Instruments and Methods in Physics Research B*, vol. 217, no. 2, pp. 276–280, 2004.

[19] M. Victoria, N. Baluc, C. Bailat et al., "The microstructure and associated tensile properties of irradiated fcc and bcc metals," *Journal of Nuclear Materials*, vol. 276, no. 1, pp. 114–122, 2000.

[20] X. Zhang, E. G. Fu, A. Misra, and M. J. Demkowicz, "Interface-enabled defect reduction in He ion irrated metallic multilayers," *JOM*, vol. 62, no. 12, pp. 75–78, 2010.

[21] A. Kashinath, A. Misra, and M. J. Demkowicz, "Stable storage of helium in nanoscale platelets at semicoherent interfaces," *Physical Review Letters*, vol. 110, Article ID 086101, 2013.

[22] S. Mao, S. Dillon, and R. S. Averback, "The influence of Cu-Nb interfaces on local vacancy concentration in Cu," *Scripta Materialia*, vol. 69, no. 1, pp. 21–24, 2013.

[23] S. Mao, S. Shu, J. Zhou, R. S. Averback, and S. J. Dillon, "Quantitative comparison of sink efficiency of Cu-Nb, Cu-V and Cu-Ni interfaces for point defects," *Acta Materialia*, vol. 82, pp. 328–335, 2015.

[24] S. J. Zinkle and N. M. Ghoniem, "Operating temperature windows for fusion reactor structural materials," *Fusion Engineering and Design*, vol. 51-52, pp. 55–71, 2000.

[25] S. J. Zinkle, "Fusion materials science: overview of challenges and recent progress," *Physics of Plasmas*, vol. 12, no. 5, Article ID 058101, 2005.

[26] M. Zhernenkov, M. S. Jablin, A. Misra et al., "Trapping of implanted He at Cu/Nb interfaces measured by neutron reflectometry," *Applied Physics Letters*, vol. 98, Article ID 241913, 2011.

[27] M. J. Demkowicz, A. Misra, and A. Caro, "The role of interface structure in controlling high helium concentrations," *Current Opinion in Solid State and Materials Science*, vol. 16, no. 3, pp. 101–108, 2012.

[28] W. Han, M. J. Demkowicz, N. A. Mara et al., "Design of radiation tolerant materials via interface engineering," *Advanced Materials*, vol. 25, no. 48, pp. 6975–6979, 2013.

[29] S. J. Zinkle and G. S. Was, "Materials challenges in nuclear energy," *Acta Materialia*, vol. 61, no. 3, pp. 735–758, 2013.

[30] G. R. Odette, M. J. Alinger, and B. D. Wirth, "Recent developments in irradiation-resistant steels," *Annual Review of Materials Research*, vol. 38, pp. 471–503, 2008.

[31] G. R. Odette and D. T. Hoelzer, "Irradiation-tolerant nanostructured ferritic alloys: transforming helium from a liability to an asset," *The Journal of The Minerals, Metals & Materials Society (TMS)*, vol. 62, no. 9, pp. 84–92, 2010.

[32] P. A. Thorsen, J. B. Bilde-Sørensen, and B. N. Singh, "Bubble formation at grain boundaries in helium implanted copper," *Scripta Materialia*, vol. 51, no. 6, pp. 557–560, 2004.

[33] M. J. Demkowicz, R. G. Hoagland, and J. P. Hirth, "Interface structure and radiation damage resistance in Cu-Nb multilayer nanocomposites," *Physical Review Letters*, vol. 100, Article ID 136102, 2008.

[34] Y. Matsukawa and S. J. Zinkle, "One-dimensional fast migration of vacancy clusters in metals," *Science*, vol. 318, no. 5852, pp. 959–962, 2007.

[35] M. J. Demkowicz, D. Bhattacharyya, I. Usov, Y. Q. Wang, M. Nastasi, and A. Misra, "The effect of excess atomic volume on He bubble formation at fcc-bcc interfaces," *Applied Physics Letters*, vol. 97, no. 16, Article ID 161903, 2010.

[36] M. J. Demkowicz, R. G. Hoagland, B. P. Uberuaga, and A. Misra, "Influence of interface sink strength on the reduction of radiation-induced defect concentrations and fluxes in materials with large interface area per unit volume," *Physical Review B*, vol. 84, Article ID 104102, 2011.

[37] L. Zhang and M. J. Demkowicz, "Morphological stability of Cu-Nb nanocomposites under high-energy collision cascades," *Applied Physics Letters*, vol. 103, no. 6, Article ID 061604, 2013.

[38] S. J. Zinkle, A. Horsewell, B. N. Singh, and W. F. Sommer, "Dispersoid stability in a Cu-Al_2O_3 alloy under energetic cascade damage conditions," *Journal of Nuclear Materials*, vol. 195, no. 1-2, pp. 11–16, 1992.

[39] X. Zhang, N. Q. Vo, P. Bellon, and R. S. Averback, "Microstructural stability of nanostructured Cu–Nb–W alloys during high-temperature annealing and irradiation," *Acta Materialia*, vol. 59, no. 13, pp. 5332–5341, 2011.

[40] M. Ames, J. Markmann, R. Karos, A. Michels, A. Tschöpe, and R. Birringer, "Unraveling the nature of room temperature grain growth in nanocrystalline materials," *Acta Materialia*, vol. 56, no. 16, pp. 4255–4266, 2008.

[41] T. Chookajorn, H. A. Murdoch, and C. A. Schuh, "Design of stable nanocrystalline alloys," *Science*, vol. 337, no. 6097, pp. 951–954, 2012.

[42] T. Höchbauer, A. Misra, K. Hattar, and R. G. Hoagland, "Influence of interfaces on the storage of ion-implanted He in multilayered metallic composites," *Journal of Applied Physics*, vol. 98, Article ID 123516, 2005.

[43] N. Li, M. S. Martin, O. Anderoglu et al., "He ion irradiation damage in Al/Nb multilayers," *Journal of Applied Physics*, vol. 105, no. 12, Article ID 123522, 2009.

[44] N. Li, E. G. Fu, H. Wang et al., "He ion irradiation damage in Fe/W nanolayer films," *Journal of Nuclear Materials*, vol. 389, no. 2, pp. 233–238, 2009.

[45] E. G. Fu, J. Carter, G. Swadener et al., "Size dependent enhancement of helium ion irradiation tolerance in sputtered Cu/V nanolaminates," *Journal of Nuclear Materials*, vol. 385, no. 3, pp. 629–632, 2009.

[46] A. Misra and H. Kung, "Deformation behavior of nanostructured metallic multilayers," *Advanced Engineering Materials*, vol. 3, no. 4, pp. 217–222, 2001.

[47] C. González, R. Iglesias, and M. J. Demkowicz, "Point defect stability in a semicoherent metallic interface," *Physical Review B*, vol. 91, Article ID 064103, 2015.

[48] M. J. Demkowicz and R. G. Hoagland, "Structure of Kurdjumov-Sachs interfaces in simulations of a copper-niobium bilayer," *Journal of Nuclear Materials*, vol. 372, no. 1, pp. 45–52, 2008.

[49] G. S. Was, *Fundamentals of Radiation Materials Science—Metals and Alloys*, Springer, Berlin, Germany, 2007.

[50] A. D. Brailsford and R. Bullough, "The rate theory of swelling due to void growth in irradiated metals," *Journal of Nuclear Materials*, vol. 44, no. 2, pp. 121–135, 1972.

[51] W. B. Krantz, *Scaling Analysis in Modeling Transport and Reaction Processes—A Systematic Approach to Model Building and the Art of Approximation*, John Wiley & Sons, New York, NY, USA, 2007.

[52] P. Zhao and Y. Shimomura, "Molecular dynamics calculations of properties of the self-interstitials in copper and nickel," *Computational Materials Science*, vol. 14, no. 1–4, pp. 84–90, 1999.

[53] W. Hu, X. Shu, and B. Zhang, "Point-defect properties in body-centered cubic transition metals with analytic EAM interatomic potentials," *Computational Materials Science*, vol. 23, no. 1–4, pp. 175–189, 2002.

[54] D. Finkenstadt, N. Bernstein, J. L. Feldman, M. J. Mehl, and D. A. Papaconstantopoulos, "Vibrational modes and diffusion of self-interstitial atoms in body-centered-cubic transition metals: a tight-binding molecular-dynamics study," *Physical Review B—Condensed Matter and Materials Physics*, vol. 74, no. 18, Article ID 184118, 2006.

[55] F. Guethoff, B. Hennion, C. Herzig, W. Petry, H. R. Schober, and J. Trampenau, "Lattice dynamics and self-diffusion in niobium at elevated temperatures," *Journal of Physics Condensed Matter*, vol. 6, no. 31, pp. 6211–6220, 1994.